Semiconductor saturable absorber mirror passively Q-switched 2.97 m fluoride fiber laser

2014 Laser Phys. Lett. 11 065102

(http://iopscience.iop.org/1612-202X/11/6/065102)

IOP Publishing | Astro Ltd
Laser Physics Letters
Laser Phys. Lett. **11** (2014) 065102 (6pp)
doi:10.1088/1612-2011/11/6/065102

Letters

Semiconductor saturable absorber mirror passively Q-switched 2.97 μm fluoride fiber laser

J F Li[1,2,3], H Y Luo[1], Y L He[1], Y Liu[1], L Zhang[2], K M Zhou[2], A G Rozhin[2] and S K Turistyn[2]

[1] State Key Laboratory of Electronic Thin Films and Integrated Devices, School of Optoelectronic Information, University of Electronic Science and Technology of China (UESTC), Chengdu 610054, People's Republic of China
[2] Institute of Photonic and Technology (AIPT), Aston University, Birmingham, UK

E-mail: lijianfeng@uestc.edu.cn

Received 14 March 2014
Accepted for publication 21 March 2014
Published 16 April 2014

Abstract
A diode-cladding-pumped mid-infrared passively Q-switched Ho^{3+}-doped fluoride fiber laser using a reverse designed broad band semiconductor saturable mirror (SESAM) was demonstrated. Nonlinear reflectivity of the SESAM was measured using an in-house Yb^{3+}-doped mode-locked fiber laser at 1062 nm. Stable pulse train was produced at a slope efficient of 12.1% with respect to the launched pump power. Maximum pulse energy of 6.65 μJ with a pulse width of 1.68 μs and signal-to-noise ratio (SNR) of ~50 dB was achieved at a repetition rate of 47.6 kHz and center wavelength of 2.971 μm. To the best of our knowledge, this is the first 3 μm region SESAM-based Q-switched fiber laser with the highest average power and pulse energy, as well as the longest wavelength from mid-infrared passively Q-switched fluoride fiber lasers.

Keywords: mid-IR fiber laser, fluoride fiber lasers, Q-switching, SESAM

(Some figures may appear in colour only in the online journal)

1. Introduction

Mid-infrared fluoride glass fiber lasers have attracted a great deal of attention in recent years because of their potential applications in defense, spectroscopy, medicine and gas sensing. In some specific applications such as material processing, micro surgery and nonlinear optical process, Q-switched fiber lasers are more desirable than continuous wave (CW) or mode-locked fiber lasers, because they can offer high energy pulses of nanosecond or microsecond pulse duration. A number of actively Q-switched Er^{3+}-doped fluoride glass fiber lasers operating on the $^4I_{11/2} \rightarrow {}^4I_{13/2}$ laser transition based on an acousto-optic modulator have been demonstrated [1–3]. Tokita *et al* demonstrated an actively Q-switched 2.8 μm Er^{3+}-doped ZBLAN fiber laser with 90 ns duration and 100 μJ pulse energy at a repetition rate of 120 kHz showing the potential for pulsed fluoride fiber lasers to achieve high pulse energy and short pulse width [3]. Compared to Er^{3+}-doped fluoride fiber laser, Ho^{3+}-doped fluoride glass fiber lasers operating on the $^5I_6 \rightarrow {}^5I_7$ laser transition have longer fluorescence wavelength offering the opportunity to extend the laser emission wavelength. Recently, we have demonstrated actively Q-switched cascaded 380 and 260 ns pulses at 3.005 and 2.074 μm with a pulse energy of 29 μJ and 7 μJ, respectively using Ho^{3+}-doped ZBLAN fiber [4], and 78 ns actively Q-switched pulses with a pulse energy of 6 μJ at 2.87 μm using Ho^{3+}/Pr^{3+} co-doped ZBLAN fiber [5].

Compared to actively Q-switched fiber lasers schemes, passively Q-switched fiber laser are more simple, compact and

[3] Author to whom any correspondence should be addressed

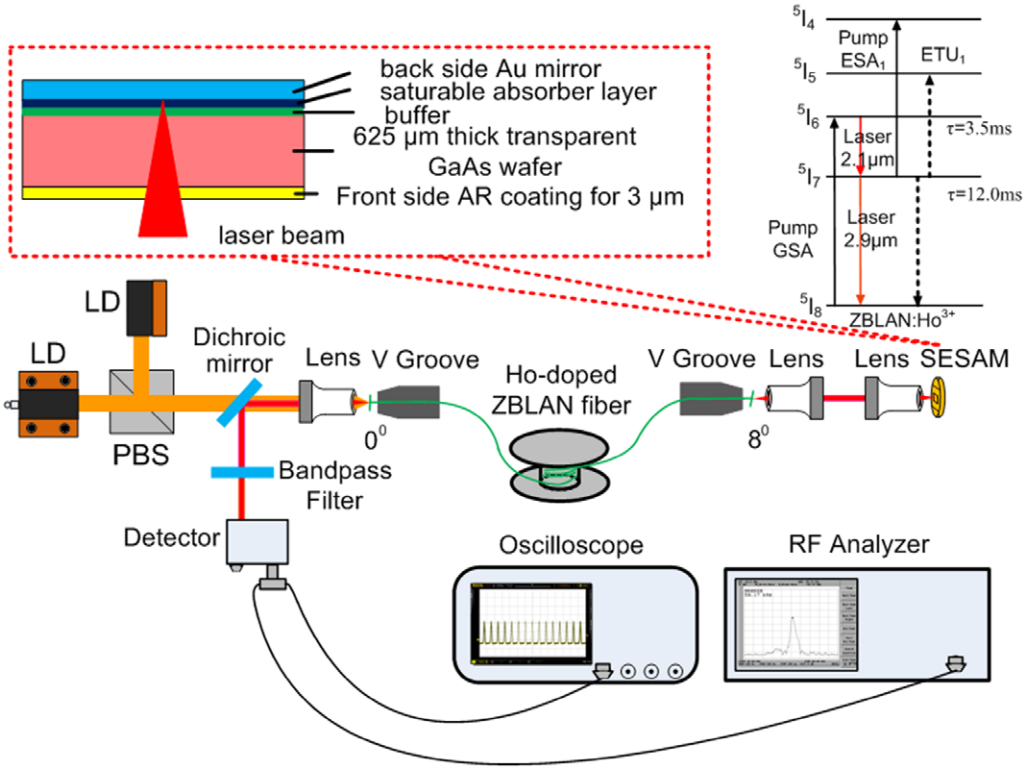

Figure 1. Schematic of the experiment setup and structure of SESAM. PBS represents polarizing beam splitter. Inset is a simplified energy-level diagram of Ho^{3+}-doped ZBLAN fiber laser including GSA, laser transition, ESA_1 and ETU_1.

cost-efficient. Several types of saturable absorber (SA) including InAs epilayers, Fe^{2+}: ZnSe crystal and graphene have been used in the mid-infrared passively Q-switched fluoride fiber lasers [6–8]. Zhu *et al* demonstrated a passively Q-switched 2.78 μm Er^{3+}-doped ZBLAN fiber laser with a pulse duration of 370 ns and a pulse energy of 2.0 μJ at a repetition rate of 161 kHz by using a Fe^{2+}:ZnSe crystal [7]. They also transferred the method to Ho^{3+}-doped ZBLAN fiber laser and achieved 2.93 μm Q-switched pulses with 800 ns pulse duration and 460 nJ pulse energy at a repetition rate of 105 kHz [8]. Using the same fiber, they also achieved Q-switched pulses with 1.2 μs pulse duration and 1 μJ pulse energy at 100 kHz repetition rate by employing a graphene deposited fiber mirror [8]. Compared to Fe^{2+}:ZnSe crystal, employing semiconductor saturable mirror (SESAM) can make the structure of laser more compact as a result of that it is reflective type of SA. Compared to graphene, it has higher damage threshold which enables higher pulse energy.

In this Letter, we report the first demonstration of a passively Q-switched Ho^{3+}-doped fluoride fiber laser using a broad band SESAM. The achieved emission wavelength and pulse energy of 2.971 μm and 6.65 μJ are also the current records produced from the mid-infrared passively Q-switched fluoride fiber lasers.

2. Experimental setup

The schematic diagram of the passively Q-switched Ho^{3+}-doped ZBLAN fiber laser is shown in figure 1. Two commercially available high power 1.15 μm diode lasers (Eagleyard Photonics, Berlin) were used to pump the fiber after polarization multiplexing and focusing into the fiber inner cladding using an antireflection-coated ZnSe objective lens (Innovation Photonics, LFO-5-6-0.975/3.0 μm, 0.25 numerical aperture (NA)) with a 6.0 mm focal length and 83% transmission at 1.15 μm. The lens was also used to collimate the 2.971 μm output laser emitted from the fiber core with a transmission of 90%. A dichroic mirror with a high transmission of 96% at 1150 nm and a reflectivity of ~95% between 2.8 and 3.1 μm was positioned between the polarizing beam splitter and the focusing lens and placed at an angle of 45° with respect to the pump beam to direct the fiber laser output. A 3 μm bandpass filter (Thorlab FB3000-500) was used to remove the residual pump light with measured transmission of ~78% at 2.971 μm. The double clad fluoride fiber with dopant concentration of 1.5 mol. % had a D-shaped pump core with a diameter of 125 μm across the circular cross section and a NA of 0.50. The fiber had a 10-μm-core diameter with an NA of 0.2. The selected fiber length of 8.0 m provided 92% pump absorption. The flat cleaved fiber end face to laser diode was used as the output coupler with ~4% Fresnel reflection. The other end of the fiber was cleaved at an angle of 8° to avoid parasitic lasing and form the single-end output ensuring most of the laser can be modulated by the SESAM. Both ends of the fiber were held by fiber holders with a V-groove (Thorlabs, HFV002) and active cooling was not necessary as a result of the low dopant concentration and long length of the fiber.

The inset of figure 1 shows the simplified energy-level scheme relevant to Ho^{3+}-doped ZBLAN fiber lasers. Pump ground state absorption (GSA) at 1150 nm excites the Ho^{3+} ions to the $^5I_6$ level. The ~3.0 μm laser transition occurs between the

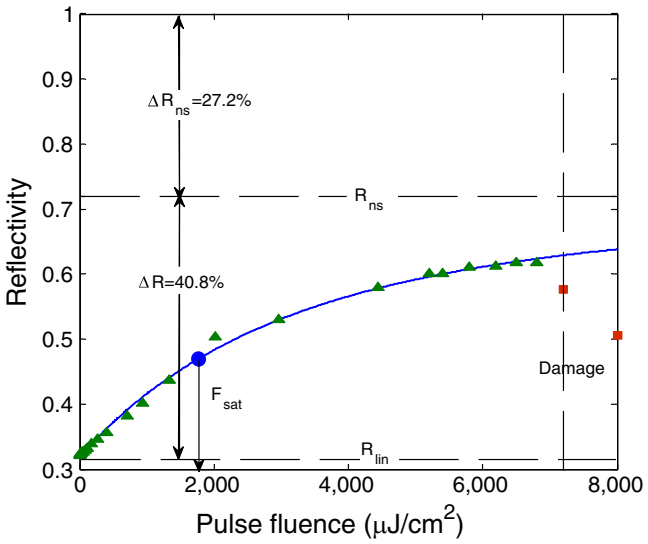

Figure 2. Measured nonlinear reflectivity of the SESAM as a function of incident pulse fluence with saturable absorption model fitting using a 1062 nm mode-locked fiber laser, where ΔR, ΔR_{ns}, R_{lin} and F_{sat} are modulation depth, non-saturable loss, low intensity reflectivity and saturation fluence, respectively. The square points represent the local damage.

$^5I_6$ and $^5I_7$ levels. However, this transition is potentially self-terminating because the shorter lifetime of the upper $^5I_6$ level [9]. Cascading the $^5I_7 \rightarrow {}^5I_8$ laser transition at a wavelength of ~2.1 μm is an effective way to de-populate the lower laser $^5I_7$ level quickly which mitigates the population bottleneck [10]. However, the threshold for 2.1 μm laser cannot be reached in our experiment due to low feedback for 2.1 μm emission at the angle cleaved fiber end and mismatch of focal point at SESAM for 2.1 and 3.0 μm emissions. In general, excited state absorption (ESA_1) at 1150 nm is helpful for depletion of the ions on the $^5I_7$ level, however, it is negligible in the cladding pumped system as a result of the low pump intensity.[12] Fortunately, the energy transfer upconversion (ETU_1) ($^5I_7$, $^5I_7 \rightarrow {}^5I_6$, $^5I_8$) can be used for depletion of the $^5I_7$ level albeit the slope efficiency is lower compared to that with cascade lasing [11].

The laser from the angled fiber end was collimated and focused onto the InAs-based SESAM (BATOP GmbH) by two ZnSe objective lenses (Innovation Photonics, LFO-5-6-3.0 μm, 0.25 NA). Compared with conventional SESAMs operating at near-infrared regime in which the distributed Bragg reflector (DBR) is sandwiched between upper absorber layers and lower GaAs substrate, the significant challenge for mid-infrared SESAM is its larger geometrical thickness of DBR structure which costs large amount of material. Particularly, the DBR operating at 3 μm needs 25 layer AlAs/GaAs pairs with a thickness of 12 μm and 24 h fabrication process at a growth rate of 0.5 μm h^{-1}. A new reverse structure with the InAs absorber layer sandwiched between upper GaAs wafer and lower Au-coated mirror instead of DBR was designed, as shown in figure 1. Good heat dissipation capability and broad operation band were obtained by using this Au-coated mirror. Note that, before growing the InAs absorber layer on the GaAs wafer, a buffer must be grown between them considering their large lattice misfit. The relaxation time and damage threshold were ~10 ps and 350 MW cm^{-1} provided by the producer [12].

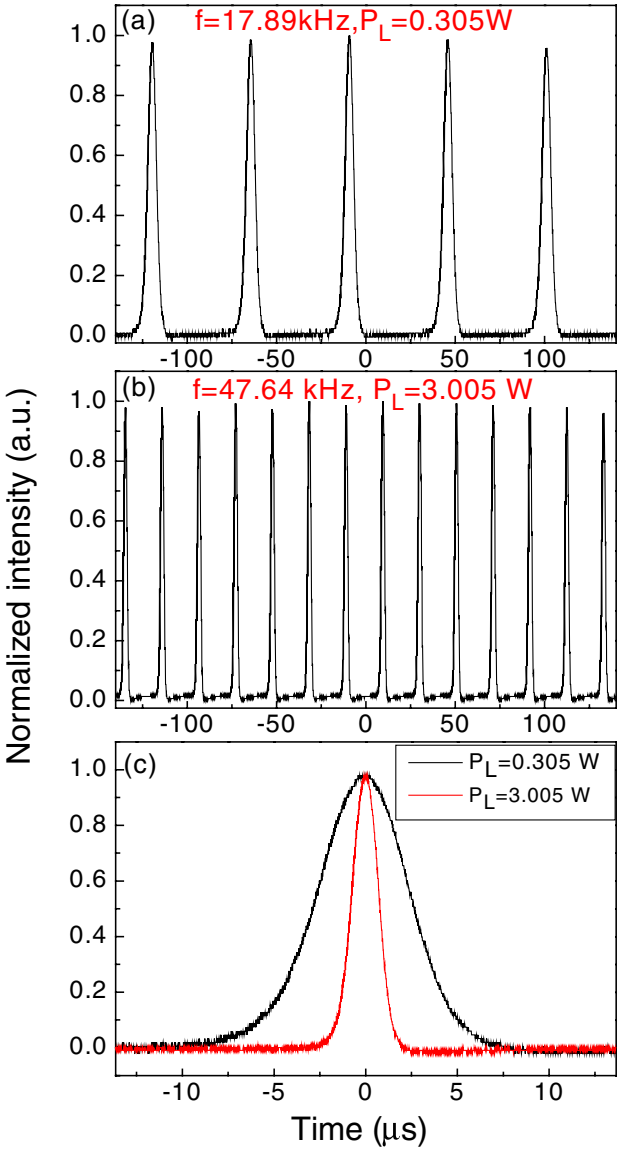

Figure 3. Q-switched pulse sequences at the launched pump power of (*a*) 0.305 W and (*b*) 3.005 W, followed with (*c*) their single pulse envelopes.

Due to lack of suitable high energy 3 μm pulsed laser source, nonlinear reflectivity of the SESAM was measured using an in-house SESAM-based mode-locked 1062 nm Yb^{3+}-doped fiber laser followed with a MOPA system. The pulse duration and repetition rate were 1.1 ps and 40 MHz, respectively. Figure 2 shows the measured nonlinear reflectivity as a function of pulse fluence with the saturable absorption model fitting as follows [13]:

$$R = 1 - \Delta R_{ns} - \Delta R \frac{1 - \exp(-F_p / F_{sat})}{(F_p / F_{sat})} \quad (1)$$

where R, ΔR_{ns}, ΔR, F_p and F_{sat} represent nonlinear reflectivity, non-saturable loss, modulation depth, incident pulse fluence and saturation fluence, respectively. Note that two phonon absorption (TPA) component was removed here since damage occurred on SESAM before TPA. Consequently, low

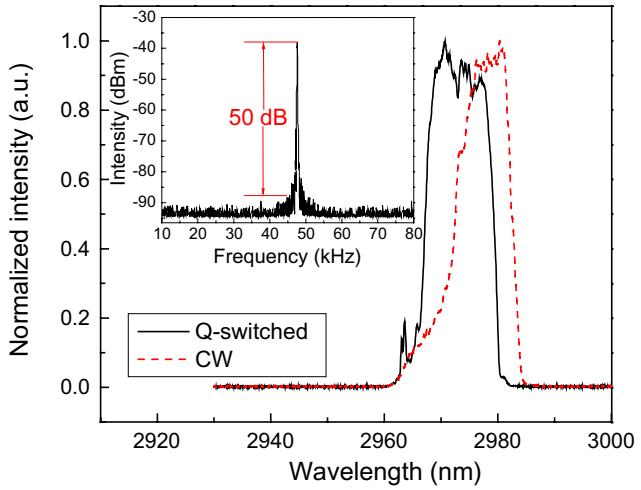

Figure 4. Measured spectra for CW and Q-switched pulsed operation at maximum launched pump power of 3.005 W. Inset is the measured fundamental RF spectrum of the laser output at a span of 70 kHz and a resolution bandwidth of 100 Hz.

intensity reflectivity R_{lin} of ~32%, modulation depth ΔR of ~40.8%, non-saturable loss ΔR_{ns} of ~27.2% and saturation fluence F_{sat} of ~1771 μJ cm^{-2} were estimated. In general, the ratio of modulation depth to non-saturated loss depends mainly on the growth temperature and slightly on the wavelength. Therefore, according to the ratio of ~1.5 (40.8/27.2%) at 1062 nm and the measured SESAM reflectivity of ~61.8% under low intensity CW laser at 2.97 μm, the modulation depth and non-saturable loss at 2.97 μm were theoretically estimated to be ~23.3% and ~15.5%, respectively. On the other hand, the saturation fluence at 2.97 μm was predicted to be much lower than that at 1062 nm laser as a result of the smaller photon energy.

The output pulsed train was measured by an InAs photodetector with a response time of approximately 2 ns connected to a 500 MHz digital oscilloscope. A monochromator with 0.005 nm resolution (Princeton instrument Acton SP2300) that employed a liquid nitrogen cooled InAs photodiode was used to measure the laser spectrum at 3 μm. An RF spectrum analyzer (Advantest R3267) with resolution bandwidth of 10 Hz to 100 MHz was used to measure the signal-to-noise ratio (SNR) of the pulses.

3. Experiment results and discussion

The CW laser was primarily generated at the launched pump power of 202 mW. After reaching the launched pump power of 235 mW, the fiber laser started to operate at the Q-switching regime, but the pulse train was unstable. When the launched pump power was increased to 305 mW, stable Q-switched pulse train was observed with a measured pulse width of 5.76 μs at a repetition rate of 17.89 kHz, as shown in figures 3(*a*) and (*c*). Then, the Q-switched pulse train can be maintained very stably to the maximum launched pump power of 3.005 W, as shown in figures 3(*b*) and (*c*), with an increasing repetition rate of up to 47.64 kHz. The pulse-to-pulse amplitude stability was approximately ±2%. The measured pulse width of 1.68 μs was longer than that reported in [4] as a result of lower pump rate and smaller modulation depth of the Q-switcher which was inversely proportional to the pulse width [14]. It is worth mentioning that we found the position of SESAM was a key factor to achieve stable Q-switching. Firstly, we adjusted the SESAM position to maximize the output power, where the focal point was on the front surface of the Au-coated mirror. However, no Q-switched pulses were observed in this case as a result of that the beam intensity on the absorber layer was not strong enough to reach the saturation intensity even at maximum pump power. Then we moved the SESAM to the lens about 2 mm, no pulses were observed during the whole range due to further decreasing of beam intensity on the absorber layer. If we moved the SESAM in the opposite direction, stable Q-switched pulses with SNR of ~35 dB occurred at ~3 μm away from the maximum power position. Further increasing the distance, the pulses became more stable and its SNR increased to the maximum of ~50 dB at ~23 μm away from the maximum power position while the average power decreased indicating the decreasing CW component. The ~23 μm was approximate the half depth of the SA layer suggesting that the laser was focused on the middle position of the absorber layer which makes more absorber operate at saturable state. Then the Q-switched pulses became weakened with decreasing output power as a further increasing of the distance, and finally disappeared after an additional ~20 μm movement.

If replacing the 8°-cleaved fiber end with a perpendicular fiber end, no Q-switched were observed at overall pump power range indicating that the Q-switched component was conquered by the CW component caused by the fiber-end-terminated cavity. Additionally if removing the collimating and focusing system after 8°-cleaved fiber end and contacting the SESAM with the fiber end directly, although Q-switched pulses can still be observed, they were not stable and even exhibited multi-pulse operation due to large amount of residual pump [15]. In this case, the Q-switched threshold was also increased compared to that employing focusing structure as a result of the increased distance between the Au-coated mirror of SESAM and fiber end introduced by the sandwiched 625 μm GaAs wafer thus decreased feedback for the divergent laser from the fiber core.

The optical spectrum of the Q-switched pulses at maximum launched pump power of 3.005 W is shown in figure 4. It is observed that the Q-switched pulse train operated at a center wavelength of 2971.45 nm with a FWHM of 12.05 nm. We replaced the SESAM by an Au-coated mirror with high reflection of >90%, the laser switched to CW regime with a red-shifted center wavelength of 2974.03 nm and compressed FWHM of 9.9 nm. The red-shifted wavelength was attributed to the Au-coated mirror induced higher feedback which decreased the laser threshold thus lowered the initial Stark level of upper laser level $^5I_6$ [10]. The inset shows the measured radio frequency (RF) spectrum of the pulse train at a span of 70 kHz and a resolution bandwidth of 100 Hz. The SNR at the launched pump power of 3.005 W is about 50 dB, which is in the typical range observed in stable Q-switched fiber lasers. Additionally, the SNR was essentially unchanged during whole range of pump power also indicating the stable Q-switched operation of our laser.

Figure 5(*a*) shows the measured repetition rate and pulse width as a function of the launched pump power. As expected,

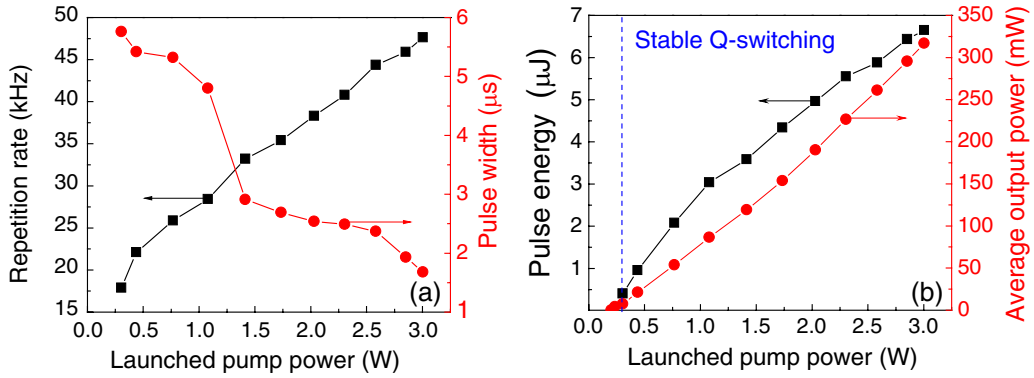

Figure 5. Measured (*a*) pulse width combined with repetition rate and (*b*) average power combined with pulse energy as a function of launched pump power.

the repetition rate increases and pulse width decreases near linearly with the increased launched pump power. The repetition rate increases from 17.89 to 47.64 kHz and pulse duration decreases from 5.76 to 1.68 μs as an increase at the launched pump power. Figure 5(*b*) shows the average output power measured and pulse energy as a function of launched pump power. The output power and pulse energy increase near linearly with increased launched pump power at a slope efficiency of 12.1% which was lower compared to cascaded Ho^{3+}-doped fluoride fiber lasers due to the lack of cascaded 2.1 μm emission [10]. At the maximum launched pump power of 3.005 W, a maximum average power of 316.7 mW and a pulse energy of 6.65 μJ only limited by the pump power were achieved. Note that the SESAM was not damaged at such a high power due to its high damage threshold and the excellent heat dissipation of the Au mirror.

In contrast to our previously SESAM mode-locked demonstration where a 3.5 m Ho^{3+}/Pr^{3+}-codoped ZBLAN gain fiber was employed [16], only Q-switched operation was achieved in this case. In order to avoid mode-locking, the following condition should be satisfied [17]:

$$\left|\frac{\mathrm{d}R}{\mathrm{d}I}\right| I > r\frac{T_\mathrm{R}}{\tau_2} \tag{2}$$

where R and I represent the SESAM reflectivity and intracavity laser intensity, respectively. r, T_R and τ_2 represent the pump to threshold ratio, cavity round trip time and upper laser state lifetime, respectively. In this case, the lower concentration Ho^{3+}ZBLAN fiber with longer length was chosen to increase the threshold. Although the T_R was increased owing to the longer cavity length, the smaller r as a result of a higher threshold, and the slightly prolonged τ_2 due to lack of Pr^{3+} ions [10] in this case decreased the right side of inequality, thus prevented the CW mode-locking operation. As described before, the minimum pulse width of 1.68 μs was only limited by the maximum pump power and the theoretical limitation was predicted to be 0.83 μs with further increased pump power according to the formula [15]:

$$\tau_\mathrm{p} = 1.76\frac{2T_\mathrm{R}}{\Delta R} \tag{3}$$

where τ_p, T_R and ΔR were limited pulse duration, cavity round trip time and modulation depth of EQ switcher, respectively.

4. Conclusion

In summary, we have demonstrated passive Q-switching of a Ho^{3+}-doped fluoride fiber laser using a new reversed design broad band InAs-based SESAM. The Q-switched pulses train with 1.68 μs duration and 316.7 mW average power was achieved at a repetition rate of 47.6 kHz. The estimated pulse energy of 6.65 μJ is the highest pulse energy from passively Q-switched 3 μm fluoride fiber lasers to our best knowledge. The 2.971 μm center wavelength of the pulse train is also the reported longest wavelength from passively Q-switched fluoride fiber lasers. Further increase in slope efficiency is possible with cascading 2 μm laser transition. Further reduction in pulse duration is expected by employing a shorter high dopant ZBLAN fiber combined with an SESAM of higher modulation depth.

Acknowledgments

The authors acknowledge useful discussions with Dr Wolfgang Richter at BATOP GmbH. This work was supported by National Nature Science Foundation of China (Grant No. 61377042, 61107037 and 61327004) and European Commission's Marie Curie International Incoming Fellowship (Grant No. 911333).

References

[1] Frerichs C and Tauermann T 1994 *IEEE Electron. Lett.* **30** 706
[2] Huber T, Lüthy W, Weber H P and Hochstrasser D F 1999 *Opt. Quant. Electron.* **31** 1171
[3] Tokita S, Murakami M, Shimizu S, Hashida M and Sakabe S 2011 *Opt. Lett.* **36** 2812
[4] Li J, Hu T and Jackson S D 2012 *Opt. Lett.* **37** 2208
[5] Hu T, Hudson D D and Jackson S D 2012 *Opt. Lett.* **37** 2145
[6] Frerichs C and Unrau U B 1996 *Opt. Fiber Technol.* **2** 358
[7] Wei C, Zhu X, Norwood R and Peyghambarian N 2012 *IEEE Photon. Technol. Lett.* **24** 1741
[8] Zhu G, Zhu X, Balakrishnan K, Norwood R and Peyghambarian N 2013 *Opt. Mater. Express* **3** 1365
[9] Librantz A F H, Jackson S D, Jagosich F H, Gomes L, Poirier G, Ribeiro S J L and Messaddeq Y 2007 *J. Appl. Phys.* **101** 123111

[10] Li J, Hudson D D and Jackson S D 2011 *Opt. Lett.* **36** 3642
[11] Li J, Gomes L and Jackson S D 2012 *IEEE J. Quantum Electron.* **48** 596
[12] www.batop.de/products/saturable absorber/saturable-absorber-mirror/data-sheet/saturable-absorber-mirror-3000nm/saturable-absorber-mirror-SAM-3000-33-10ps.pdf
[13] Okhotnikov O, Grudinin A and Pessa M 2004 *New J. Phys.* **6** 177
[14] Braun B, Kärtner F X, Zhang G, Moser M and Keller U 1997 *Opt. Lett.* **22** 381
[15] Yang W, Hou J, Zhang B, Song R and Liu Z 2012 *Appl. Opt.* **51** 5664
[16] Li J, Hudson D D, Liu Y and Jackson S D 2012 *Opt. Lett.* **37** 3747
[17] Keller U, Weingarten K J, Kartner F X, Kopf D, Braun B, Jung I D, Fluck R, Honninger C, Matuschek N, Aus der Au J 1996 *IEEE J. Sel. Top. Quantum Electron.* **2** 435